

Testicular Architecture Is Critical for Mediation of Retinoic Acid Responsiveness by Undifferentiated Spermatogonial Subtypes in the Mouse

Tessa Lord,¹ Melissa J. Oatley,¹ and Jon M. Oatley^{1,*}

¹School of Molecular Biosciences, Centre for Reproductive Biology, College of Veterinary Medicine, Washington State University, Pullman, WA 99164, USA

*Correspondence: joatley@vetmed.wsu.edu

<https://doi.org/10.1016/j.stemcr.2018.01.003>

SUMMARY

Spermatogenesis requires retinoic acid (RA) induction of the undifferentiated to differentiating transition in transit amplifying (TA) progenitor spermatogonia, whereas continuity of the spermatogenic lineage relies on the RA response being suppressed in spermatogonial stem cells (SSCs). Here, we discovered that, in mouse testes, both spermatogonial populations possess intrinsic RA-response machinery and exhibit hallmarks of the differentiating transition following direct exposure to RA, including loss of SSC regenerative capacity. We determined that SSCs are only resistant to RA-driven differentiation when situated in the normal topological organization of the testis. Furthermore, we show that the soma is instrumental in “priming” TA progenitors for RA-induced differentiation through elevated RA receptor expression. Collectively, these findings indicate that SSCs and TA progenitor spermatogonia inhabit disparate niche microenvironments within seminiferous tubules that are critical for mediating extrinsic cues that drive fate decisions.

INTRODUCTION

Gametes are the eternal link between generations and are key to the continuation and diversity of animal populations. In mammalian males, continual spermatogenesis is required for fertility, generating millions of genetically unique spermatozoa daily. Both the robustness and continuity of this process is reliant on a small pool of spermatogonial stem cells (SSCs) that are rare in number, estimated to comprise 0.01%–1% of the total testis cell population depending on the species (Tegelenbosch and de Rooij, 1993). In mice, the SSC pool is thought to exist as a subset of the A_{single} spermatogonial population closely associated with the basement membrane of the seminiferous tubules (reviewed by Lord and Oatley, 2017). These A_{single} SSCs undergo mitotic proliferation in order to achieve self-renewal, or alternatively, to produce transit amplifying (TA) progenitor cells that no longer possess stem cell capacity and undergo clonal expansion, remaining connected by intercellular bridges to produce chains ranging from 2 (A_{paired}) to 16 cells (A_{aligned}). A round of spermatogenesis is initiated when a pulse of retinoic acid (RA) induces a majority of the TA progenitor spermatogonia to transition from the undifferentiated type A to differentiating type A1 state. In support of the A_{single} model (Huckins, 1971; Oakberg, 1971), and more recently the “revised A_{single} model” (de Rooij, 2017; Lord and Oatley, 2017), the propensity for spermatogonia to respond to the RA signal is directly proportional to chain length, with ~88% of the undifferentiated spermatogonial population undergoing the A to A1 transition in response to RA, including 63% of A_{paired} , 95% of $A_{\text{aligned}4}$, and 100% of $A_{\text{aligned}8-16}$, while none of the A_{single} spermatogonia make the differentiating transition. Importantly, SSCs must be resistant to the RA signal

or the foundation for continuity of the spermatogenic lineage will be lost (Ikami et al., 2015; Tegelenbosch and de Rooij, 1993).

While it has long been established that RA signaling is absolutely required for spermatogenesis (van Pelt and de Rooij, 1990; Wolbach and Howe, 1925), with vitamin A-deficient models experiencing infertility by consequence of a loss of the differentiating spermatogonial pool (Li et al., 2011), the mechanisms by which SSCs resist the differentiating signal that influences closely situated progenitors remains unresolved. A recent study by Ikami et al. (2015) proposed that responsiveness or resistance to RA signaling in spermatogonia is dictated by “on” or “off” expression of the retinoic acid receptor (RAR) variant γ . In that study, the “SSC” pool was considered to be all cells expressing the glial cell line-derived neurotrophic factor (GDNF) family receptor $\alpha 1$ (GFRA1), while the TA progenitor pool was identified as the Neurogenin3 (NEUROG3) expressing population of spermatogonia. Based on immunohistochemical analyses, the GFRA1+ population was described as having little to no RAR γ expression, while RAR γ expression in the NEUROG3+ progenitors was high. Although these findings imply a simple hierarchical classification of spermatogonia as RA-resistant SSCs and RA-responsive progenitors, it is at odds with other findings, and does not necessarily fit with known dynamics of the spermatogonial-soma interactions in mammalian testes. First, studies by Gely-Pernot et al. (2012) demonstrated that conditional ablation of *Rarg* within the spermatogonial population specifically is insufficient to block the differentiating transition, that expression of RAR γ is evident in a portion of the GFRA1+ spermatogonial population, and that induction of classical RA-responsive genes *Stra8* (stimulated by retinoic acid 8) and *Kit* (KIT proto-oncogene receptor tyrosine kinase) can





be achieved via both the RAR γ and RAR α variants in spermatogonia. Indeed, widespread impediment of spermatogonial responsiveness to RA signaling was only observed when expression of both *Rar α* and *Rar γ* were ablated conditionally in spermatogonia (Gely-Pernot et al., 2012). Second, several previous studies have demonstrated that GFRA1+ and NEUROG3+ spermatogonial populations are not mutually exclusive as SSCs and TA progenitors, respectively (Buageaw et al., 2005; Ebata et al., 2005; Grisanti et al., 2009; Yoshida et al., 2004) (expression profiles of all markers discussed/utilized in this study are depicted in Figure S1). Third, both *Rar γ* and *Rar α* gene expression is detectable in Inhibitor of DNA binding 4 (ID4)-eGFP+ and ID4-eGFP- spermatogonial populations that are highly enriched for SSCs and progenitors, respectively (Chan et al., 2014). Lastly, the hierarchical model proposed by Ikami et al. eliminates an influence from the soma in modulating the RA response in spermatogonia, which is at odds with the well-established dynamic role that multiple testis somatic cell populations play in the biosynthesis and clearance of RA (Hogarth et al., 2015; Kent et al., 2015; Tong et al., 2013).

Here, we aimed to further clarify the modes by which RA signaling is modulated in spermatogonial subtypes to preserve the SSC pool and therefore continuity of the spermatogenic lineage. Using the *Id4-eGfp* transgenic mouse model in which the ID4-eGFP+ cells are SSCs and ID4-eGFP- cells are mostly progenitors (Chan et al., 2014; Hessel et al., 2017b), RAR α and RAR γ expression was detected at similar levels in both populations of spermatogonia from testes and primary cultures. In addition, we found expression of both RAR α and RAR γ in GFRA1+ spermatogonia. Using primary cultures of undifferentiated spermatogonia that consist of SSCs and progenitors, we found that direct exposure to RA elicits hallmark responses of the differentiating transition in both populations and functional transplantation analyses confirmed depletion of the SSC pool. Lastly, we found that intricate niche microenvironments created by the soma in the testis work to simultaneously protect the SSCs from exogenous RA, while priming progenitors to be highly responsive to the RA pulse. Taken together, these findings support an adapted model for modulation of RA responsiveness in mammalian testes for which the soma is key to preservation of the SSC pool during successive rounds of spermatogenesis.

RESULTS

Expression of RAR/RXR Isoforms in SSC and TA Progenitor Populations

RA signaling is mediated by heterodimers of RARs and RXRs, each consisting of α , β , and γ variants. In order to compare expression profiles for these isoforms in highly

enriched SSC and progenitor populations, we utilized primary cultures of undifferentiated spermatogonia generated from *Id4-eGfp* transgenic mice (Chan et al., 2014). In previous studies that used RNA sequencing (RNA-seq) to compare ID4-eGFP+/SSC and ID4-eGFP-/progenitor populations, we identified similar transcript levels for *Rar α* , *Rar γ* , *Rxr α* , and *Rxr β* (Chan et al., 2014) (fragments per kilobase of transcript per million fragments mapped values provided in Figure S2B). In the current study, we validated these findings using RT-PCR (Figure S2A). Also, in agreement with other studies that explored the spermatogonial population overall (Gely-Pernot et al., 2012, 2015; Ghysselinck et al., 1997), we confirmed that expression of *Rar β* and *Rxr γ* is not detectable in cultured spermatogonia (Figure S2A). Further, using western blot analyses to assess expression of these factors at the protein level, we found expression of RAR α (55 kDa), RAR γ (58 kDa), RXR α (53–60 kDa), and RXR β (57 kDa) in both ID4-eGFP+/SSC and ID4-eGFP-/progenitor populations from primary pup cultures (Figure 1A). Next, we explored whether the expression profile of RARs/RXRs in cultures derived from pups was similar in those derived from adult mice. In agreement with data generated using the post-natal day (P) 6–8 pup cultures, expression of RAR α , RAR γ , RXR α , and RXR β was detected in ID4-eGFP+/SSC and ID4-eGFP-/progenitor populations in adult cultures, as depicted by both RT-PCR and Western blot analyses (Figures S2C and 1A).

Considering that a period of *in vitro* maintenance could have altered expression profiles, we next aimed to determine whether the RAR/RXR variants are expressed by the SSC population *in vivo*. The outcomes of RT-PCR and Western blot analyses confirmed that RAR α , RAR γ , RXR α , and RXR β are all expressed by ID4-eGFP+/SSCs isolated directly from P6–8 testes (Figures S2C and 1B). Note that examination of ID4-eGFP- spermatogonia in testes is challenging because, unlike the ID4-eGFP- population from primary cultures of undifferentiated spermatogonia, fluorescence-activated cell sorting (FACS) directly from the testis also yields somatic cells and differentiating spermatogonia that are known to express RARs and RXRs (Chan et al., 2014; Hessel et al., 2017b). Thus, we were unable to compare expression profiles between ID4-eGFP+ and ID4-eGFP- population in testes. Similarly, our ability to assess expression in ID4-eGFP+ spermatogonia from adult testes using cell sorting is limited by an ID4-eGFP fluorescence signal in spermatocytes (Chan et al., 2014). Thus, in conjunction with Western blot and RT-PCR analyses of cells isolated from cultures or pup testes directly, *in situ* assessment by immunofluorescence staining was used to confirm expression of RAR α/γ and RXR α/β in ID4-eGFP+ spermatogonia in cross-sections of testes from both P6 and adult mice (Figure 1C, arrows). As expected,

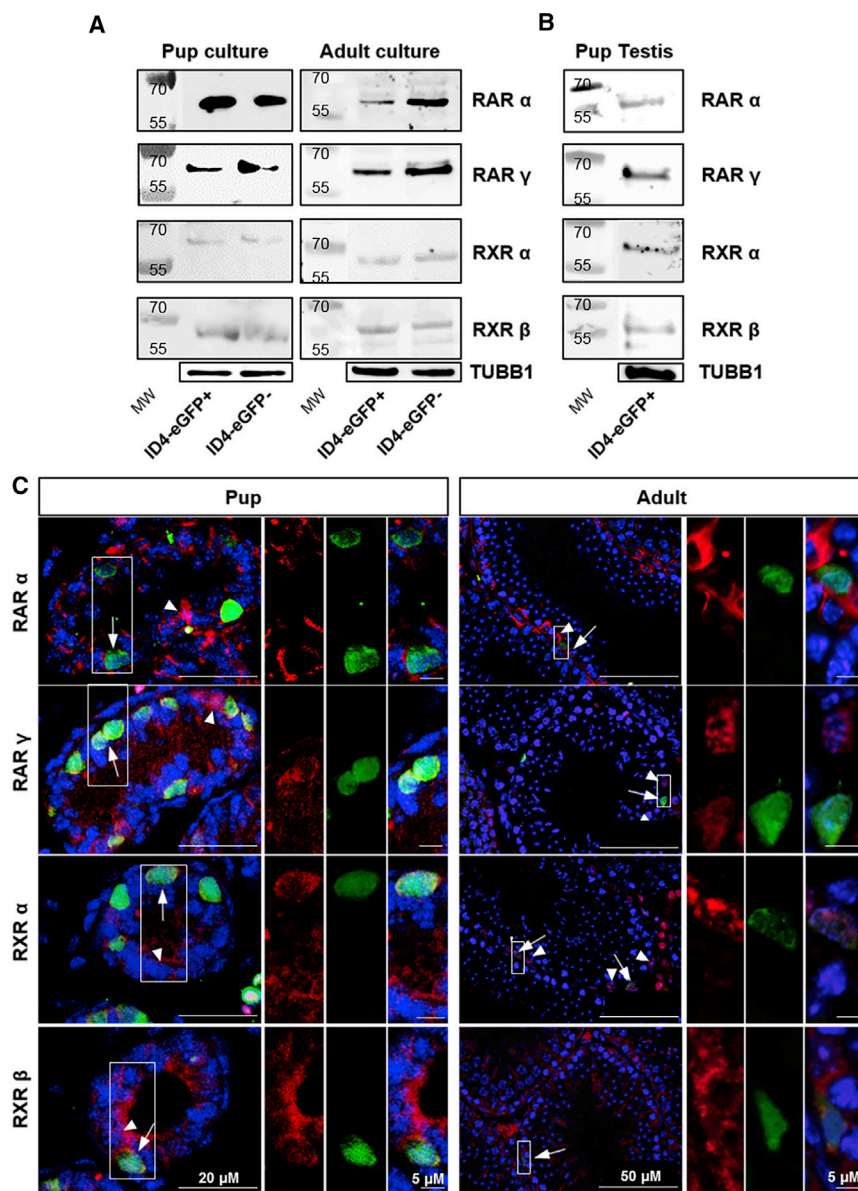


Figure 1. Expression of RAR and RXR Variants in both SSC and Progenitor Spermatogonial Populations

(A and B) Representative images of Western blot analyses for RAR α , RAR γ , RXR α , and RXR β in ID4-eGFP $^{+}$ and ID4-eGFP $^{-}$ populations in primary cultures of spermatogonia established from P6–8 pup or adult mice (A) and ID4-eGFP $^{+}$ spermatogonia isolated directly from the testes of pups (B). Tubulin (TUBB1) loading controls are included beneath each image.

(C) Representative images of immunostaining for expression of RAR α , RAR γ , RXR α , and RXR β by ID4-eGFP $^{+}$ and ID4-eGFP $^{-}$ spermatogonia in cross-sections of testes from pups and adult mice. Arrows and arrowheads indicate ID4-eGFP $^{+}$ or ID4-eGFP $^{-}$ spermatogonia co-expressing RAR α , RAR γ , RXR α , or RXR β , respectively. Boxed regions are magnified in images to the right. Negative controls are presented in Figure S2.

RAR/RXR expression was also identified in ID4-eGFP $^{-}$ spermatogonia (Figure 1C, arrowheads), throughout the nucleus and cytoplasm (Figures 1C and S3B). Images of negative control sections with normal immunoglobulin G (IgG) as the primary antibody are presented in Figure S3A. Sub-cellular localization of RARs was further visualized in ID4-eGFP $^{+}$ /SSCs and ID4-eGFP $^{-}$ /progenitors in immunocytochemistry experiments performed on spermatogonia taken from primary cultures (depicted in Figure S3B). Further examples of RAR expression in the testis have been provided using the undifferentiated spermatogonia marker LIN28 (Figure S1), with distinct overlay being evident between LIN28 and RAR expression (Figure S3C).

Lastly, we explored whether the expression of RAR and RXR isoforms by spermatogonia with stem cell characteristics is unique to the ID4-eGFP $^{+}$ population. Based on the outcomes of immunostaining analyses, a recent study reported that RAR γ is not expressed by GFRA1 $^{+}$ spermatogonia, which have also been considered to represent the SSC pool (Ikami et al., 2015). Here, we aimed to confirm this finding using different approaches. First, using flow cytometric analysis we found that the vast majority of ID4-eGFP $^{+}$ /SSCs (including both ID4-eGFP $^{\text{Bright}}$ and ID4-eGFP $^{\text{Dim}}$ subsets of the population) in primary cultures of spermatogonia, and directly from the pup testis, are GFRA1 $^{+}$, implying that the population does express

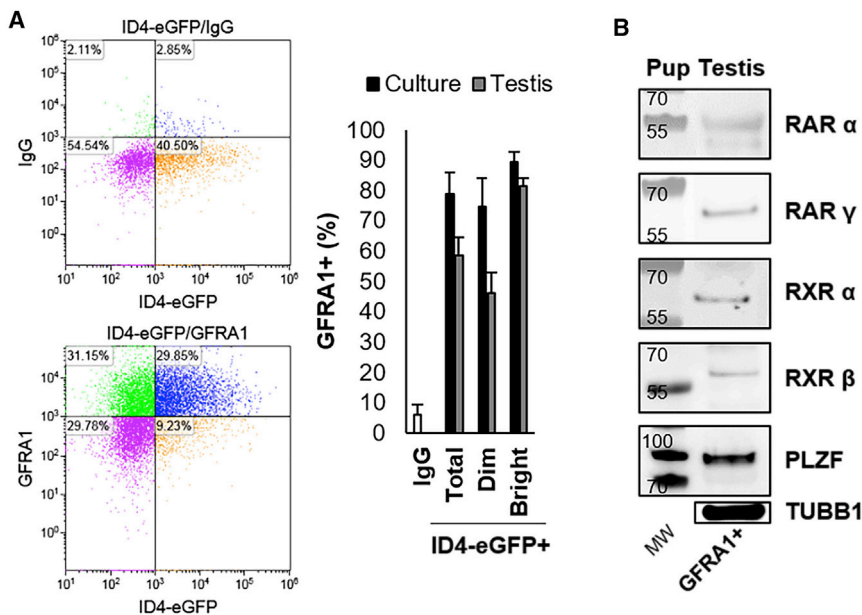


Figure 2. RAR/RXR Variants Are Expressed in the GFRA1+ Spermatogonial Population

(A) Quantification of the percentage of the ID4-eGFP⁺, ID4-eGFP^{Bright}, and ID4-eGFP^{Dim} populations that are GFRA1⁺ in primary cultures of undifferentiated spermatogonia and in pup testes using FACS analysis (representative images on left). Data are mean \pm SEM for n = 3 different cultures or animals (biological replicates).

(B) Representative images of western blot analyses for RAR α , RAR γ , RXR α , and RXR β in the GFRA1⁺ population isolated directly from pup testis. PLZF expression was assessed to confirm successful isolation of the undifferentiated spermatogonia population. Tubulin (TUBB1) expression was used as a loading control.

RARs/RXRs (Figure 2A). Indeed, these findings are aligned with those in the literature in which ID4 and GFRA1 expression are highly analogous (Helsel et al., 2017b; Chan et al., 2014) (depicted in Figure S1). Second, using western blot analysis of FACS-isolated populations from testes of P6–8 mice we found that the GFRA1⁺ population expresses RAR α , RAR γ , RXR α , and RXR β , similar to the ID4-eGFP⁺ population (Figure 2B). Taken together, these results suggest that both SSC and progenitor populations express a receptor complement for induction of RA signaling, and, thus, differential expression is unlikely to account for the resistance of SSCs to RA-induced differentiation *in vivo*. Importantly, it should be noted that the RAR γ antibody used in this study has been subjected to stringent validation, and does not react with cells in testes of *Rar γ* null mice (Gely-Pernot et al., 2015).

Activation of RA Signaling in SSC and Progenitor Populations

Considering that both SSC and progenitor spermatogonial populations in cultures and testes express RA receptors, we next aimed to assess whether this is sufficient to elicit a signaling response in both populations, and whether small fluctuations in RAR/RXR expression between SSC and progenitor subsets seen in Figure 1A translate to a differential RA response. To test this with direct exposure to RA, primary cultures of undifferentiated spermatogonia established from either pup (P6–8) or adult *Id4-eGfp* transgenic mice were treated with 0.5 μ M all-*trans* RA or vehicle (DMSO) for 16 hr as described previously (Yang et al., 2013), followed by examination of the expression level of the RA-responsive genes *Stras8* and *Kit* across ID4-eGFP⁺/

SSC and ID4-eGFP⁻/progenitor populations. In these experiments, we reasoned that, if an intrinsic mechanism acts to block the RA response in SSCs, suppressed or reduced expression of RA-responsive genes would occur in the ID4-eGFP⁺ population compared with the ID4-eGFP⁻ progenitors. Alternatively, if the RA response is blocked/prevented in SSCs by action of extrinsic factors in the niche, we would expect that direct exposure to RA *in vitro* would stimulate an equivalent STRA8/KIT response to that seen in the ID4-eGFP⁻/progenitor pool.

Using qRT-PCR analysis, we measured a significant ($p < 0.01$) induction of both *Stras8* and *Kit* gene expression in ID4-eGFP⁺ and ID4-eGFP⁻ populations of pup and adult cultures (n = 4 for each age) treated with RA compared with DMSO (Figures 3A and 3B). Furthermore, no difference in the level of induction between the two populations was measured for either of the parameters examined. These findings were further supported via analysis of STRA8 and KIT expression at the protein level. Based on immunocytochemical staining, 73% ($\pm 13.5\%$) and 61.3% ($\pm 7.0\%$) of the ID4-eGFP⁺ population in pup and adult cultures, respectively, were found to be STRA8⁺ at 16 hr post-RA treatment, which was not significantly different ($p > 0.05$) compared with the 67.5% ($\pm 7.1\%$) and 57.0% ($\pm 1.0\%$) of the ID4-eGFP⁻ populations in pup and adult cultures, respectively (Figures 3C and S4A). The percentage of cells that were STRA8⁺ in all cultures treated with DMSO was negligible. Using flow cytometric analysis, we measured a significant ($p < 0.05$) increase in KIT⁺ cells for both ID4-eGFP⁺ and ID4-eGFP⁻ populations treated with RA compared with DMSO (Figure 3D). In cultures derived from pups (n = 5), 49.0% ($\pm 11.6\%$) of ID4-eGFP⁺ and 47.5% ($\pm 11.4\%$) of

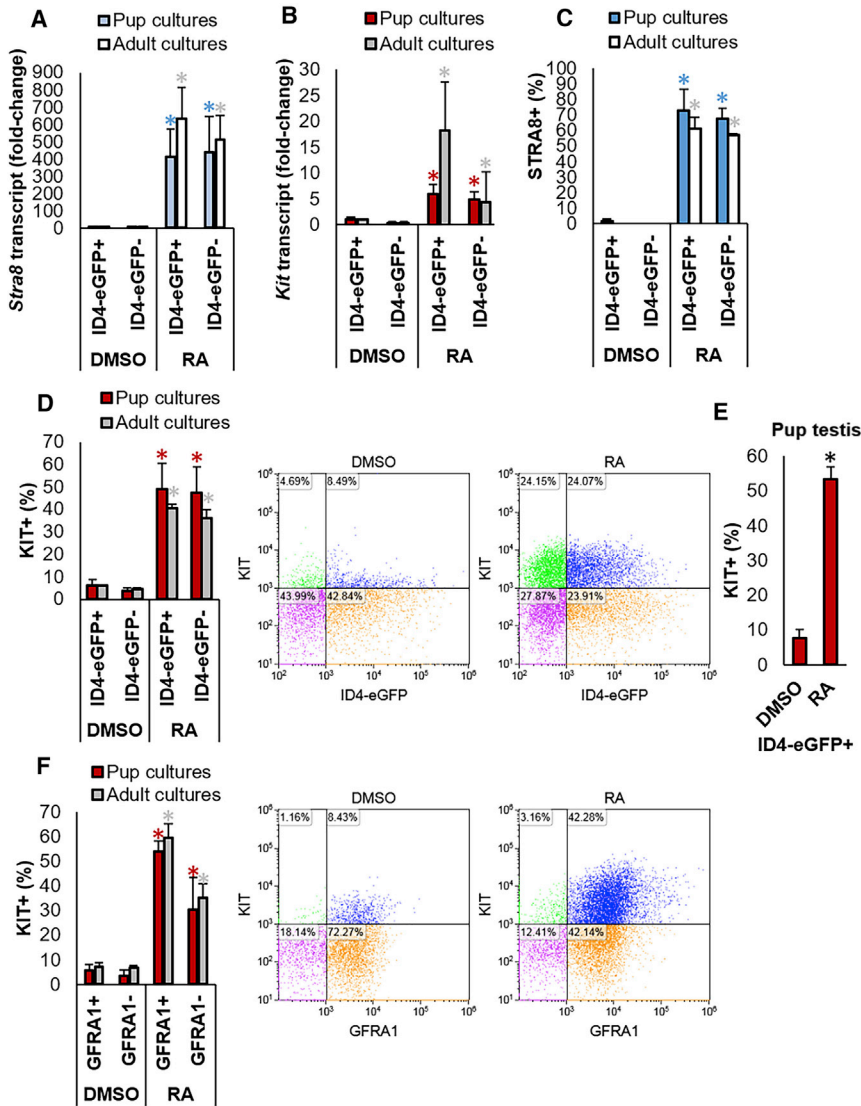


Figure 3. Responsiveness of SSC and Progenitor Spermatogonia to Direct RA Exposure In Vitro

(A and B) qRT-PCR analysis for relative *Stra8* (A) and *Kit* (B) gene expression in ID4-eGFP+/SSC and ID4-eGFP-/progenitor populations of primary undifferentiated spermatogonial cultures established from P6–8 pups (blue or red bars, respectively) or adult (white or gray bars, respectively) mice treated with DMSO (control) or all-*trans* retinoic acid (RA). Both genes are hallmark responders of the RA signaling response in spermatogonia. Data are mean \pm SEM for $n = 3$ different cultures (biological replicates). *Significantly different at $p < 0.05$ from DMSO control.

(C and D) Quantification of the percentage of ID4-eGFP+/SSC and ID4-eGFP-/progenitor cells in primary undifferentiated spermatogonial cultures established from pup or adult mice expressing STRA8 (C) or KIT (D) protein following DMSO (control) or RA treatment. Data were generated by immunocytochemical staining (STRA8+ cells, representative images provided in Figure S3) or flow cytometric analysis (KIT+ cells, representative histograms provided in D) of single-cell suspensions and are presented as mean \pm SEM for $n = 3$ different cultures (biological replicates). *Significantly different at $p < 0.05$ from DMSO control.

(E) Quantification of the percentage of KIT+ cells in the ID4-eGFP+ population isolated from pup testes and treated with DMSO (control) or RA. Data are mean \pm SEM for cell from $n = 3$ different animals. *Significantly different at $p < 0.05$ from DMSO control.

(F) Quantification of the percentage of KIT+/GFRA1+ cells in primary cultures of undifferentiated spermatogonia established from pup or adult mice following treatment with DMSO (control) or RA. Data were generated from flow cytometric analysis (representative scatterplots are presented) and are mean \pm SEM for $n = 3$ different cultures (biological replicates). *Significantly different at $p < 0.05$.

ID4-eGFP- cells were KIT+ following RA exposure representing an 8- and 12-fold increase compared with DMSO treatment, respectively. For cultures derived from adult mice, 40.7% ($\pm 1.7\%$) and 36.1% ($\pm 3.8\%$) of cells were found to be KIT+ after RA treatment, representing a 7- and 8-fold increase compared with DMSO treatment, respectively. As with STRA8 expression, no significant differences ($p > 0.05$) in the percentage of KIT+ cells were detected between RA-treated ID4-eGFP+ and ID4-eGFP- populations for both pup and adult cultures. Next, we examined whether the RA response in the SSC population was an artifact associated with long-term *in vitro* culture. To achieve this, the SSC-enriched ID4-eGFP+ population was

isolated from testes of P6–8 mice and subjected to an identical treatment regimen. Similar to cultured cells, 53.5% ($\pm 3.6\%$) of the ID4-eGFP+ cells became KIT+ following RA exposure, compared with only 7.6% ($\pm 2.6\%$) of the population following DMSO treatment (Figure 3E). Lastly, we explored whether these results are unique to the ID4-eGFP+ population by examining GFRA1+ cells, which are often considered to also represent the SSC pool and have been reported to be refractory to RA exposure (Ikami et al., 2015). Using flow cytometric analysis for KIT+ cells, we found that 54.0% ($\pm 5.6\%$) and 59.7% ($\pm 4.4\%$) of GFRA1+ cells were KIT+ after RA exposure in pup ($n = 3$) and adult ($n = 3$) cultures, respectively, which was

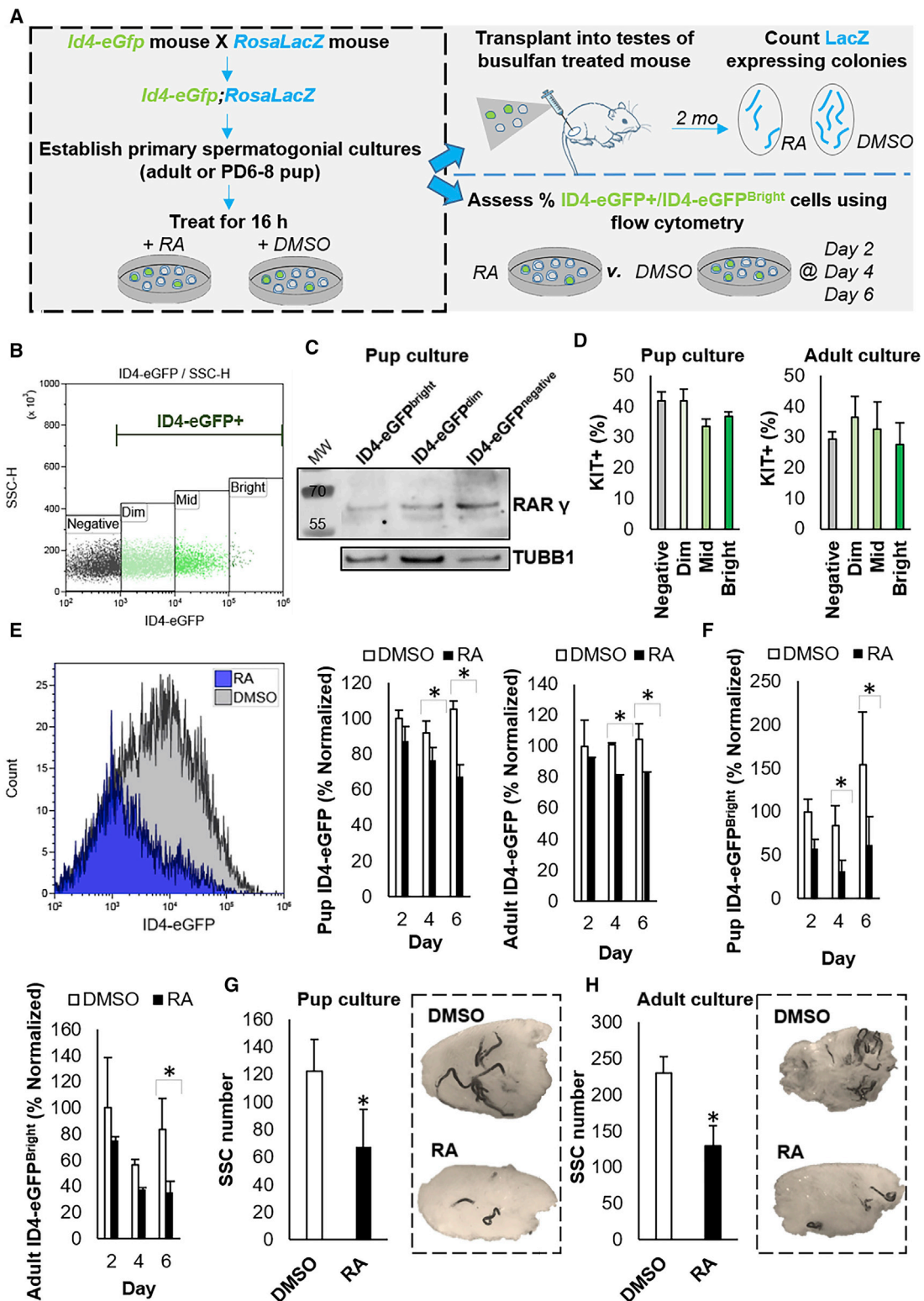


Figure 4. Impact of Direct Exposure to RA on Regenerative Capacity of the SSC Population

(A) Experimental scheme for assessing changes in SSC content of primary undifferentiated spermatogonial cultures following direct exposure to RA. Note that all spermatogonia from the culture well (*ID4-eGFP*⁺ and *ID4-eGFP*⁻) were subjected to DMSO or RA treatment.

(legend continued on next page)



significantly ($p < 0.01$) increased compared with the 5.6% ($\pm 1.7\%$) and 7.0% ($\pm 2.4\%$) of KIT⁺ cells in DMSO-treated cultures, respectively (Figure 3F).

Collectively, these findings confirm that not only are RARs and RXRs expressed in SSC and TA progenitor spermatogonial subsets, but the signaling pathway is functionally intact. Further, these results suggest that the resistance of SSCs to RA-induced differentiation *in vivo* is reliant on these cells being situated within a protective niche, and that intrinsically expressed factors are not sufficient for blocking the RA response. Notably, the trends are not unique to the dose of RA utilized because an equivalent KIT response occurs in ID4-eGFP⁺ and ID4-eGFP⁻ populations at a range of RA concentrations; from 0.5 μ M to 0.5 fM, with a stepwise reduction in the percentage of KIT⁺ cells with each reduction in RA concentration (Figure S5).

Alteration of SSC Functionality following Direct Exposure to RA

Next, we aimed to assess whether the activation of RA signaling responses in SSCs leads to a change in function. The experimental scheme is presented in Figure 4A. Because the percentage of undifferentiated spermatogonia that are ID4-eGFP⁺ is reflective of SSC content, both *in vitro* (Chan et al., 2014) and *in vivo* (Helsel et al., 2017b), we first decided to measure fluctuations in the pool in response to direct RA exposure. As reported previously (Helsel et al., 2017b), fluorescent intensity in the ID4-eGFP⁺ population can be subdivided into quadrants of Bright, Mid, Dim, and Negative in primary cultures derived from pups, and we observed a similar profile for cultures derived from adult cells (Figure 4B). In addition, we previously demonstrated that the density of cells with regenerative capacity *in vivo* is greatest in the ID4-eGFP^{Bright} population (Helsel et al., 2017b). Thus, to ensure that our findings in the ID4-

eGFP⁺ population reflect that of the ID4-eGFP^{Bright} population, we confirmed RAR/RXR expression in ID4-eGFP^{Bright} cells from primary culture using Western blot analysis (Figures 4C and S3D). It should be noted that it was not possible to compare RAR/RXR expression in ID4-eGFP^{Bright} versus ID4-eGFP^{Dim} spermatogonia using an immunohistochemistry approach as, post-fixation, distinguishing between these “levels” of ID4-eGFP fluorescence is not possible. In support of our Western blotting analysis, however, acquisition of KIT expression following RA treatment ($n = 3$ cultures examined) was largely equivalent in ID4-eGFP^{Bright}, Mid, and Dim populations of primary cultures established from either pup or adult cells (Figure 4D).

In order to track an impact of direct exposure to RA on functional changes of the SSC pool, we first assessed alteration of the ID4-eGFP⁺ population at 2, 4, and 6 days post-RA or -DMSO treatment of the entire undifferentiated spermatogonial population within the culture well. A significant ($p < 0.01$) reduction in the percentage of the overall ID4-eGFP⁺ population in primary cultures of spermatogonia established from pups and adult mice ($n = 3$) was measured in RA-treated cells compared with DMSO-treated cells at day 4 and 6 (Figure 4E). Likewise, the percentage of ID4-eGFP^{Bright} cells was significantly ($p < 0.05$) diminished following RA exposure at 4 and 6 days post-RA treatment (Figure 4F). Second, we carried out transplantation analyses to assess alteration in the regenerative stem cell content of cultures following RA treatment. Outcomes aligned with changes in the ID4-eGFP^{Bright} population (Figures 4G and 4H), in that the number of donor-derived spermatogenic colonies was significantly ($p < 0.05$) reduced in cultures treated with RA (67.8 ± 26.9 colonies/ 10^5 cells for pup cultures and 130.2 ± 24.7 colonies/ 10^5 cells for adult cultures) following as little as 16 hr exposure compared with DMSO-treated cultures (122.5 ± 22.7 colonies/ 10^5 cells for pup

(B) Representative scatterplot for the ID4-eGFP⁺ population in primary cultures of undifferentiated spermatogonia. The population can be subdivided based on Bright, Mid, Dim, and Negative EGFP intensity and the SSC population is mostly contained in the ID4-eGFP^{Bright} subset.

(C) Representative image of western blot analysis for RAR γ expression in ID4-eGFP^{Bright}, Dim, and Negative spermatogonial pools from primary cultures. Tubulin (TUBB1) expression was used as a loading control.

(D) Quantification of KIT⁺ cells in the ID4-eGFP subpopulations following direct exposure to RA. Data are presented mean \pm SEM for $n = 3$ different cultures established from 3 independent P6–8 pups or adult mice.

(E) Quantification of the percentage of cells that could be classified as ID4-eGFP⁺ in pup- or adult-derived primary cultures at 2–6 days after treatment with DMSO (control) or RA. Data were generated from flow cytometric analyses (representative histogram plot is presented) and are presented as mean \pm SEM for $n = 3$ different cultures (biological replicates).

(F) Quantification of the percentage of cells in primary cultures established from pup or adult mice that were ID4-eGFP^{Bright} at 4 and 6 days after treatment with DMSO (control) or RA. Data were generated by flow cytometric analysis and are presented as mean \pm SEM for $n = 3$ different cultures (biological replicates).

(G and H) Quantification of SSC number (donor-derived colonies of spermatogenesis/ 10^5 cells transplanted) in primary cultures established from (G) pup or (H) adult mice, transplanted 16 hr after treatment with DMSO (control) or RA. Data were generated by functional transplantation analyses (representative images of recipient testes with *LacZ*-stained donor-derived spermatogenic colonies are presented) and are mean \pm SEM for $n = 3$ different cultures (biological replicates).

*Significantly different at $p < 0.05$.

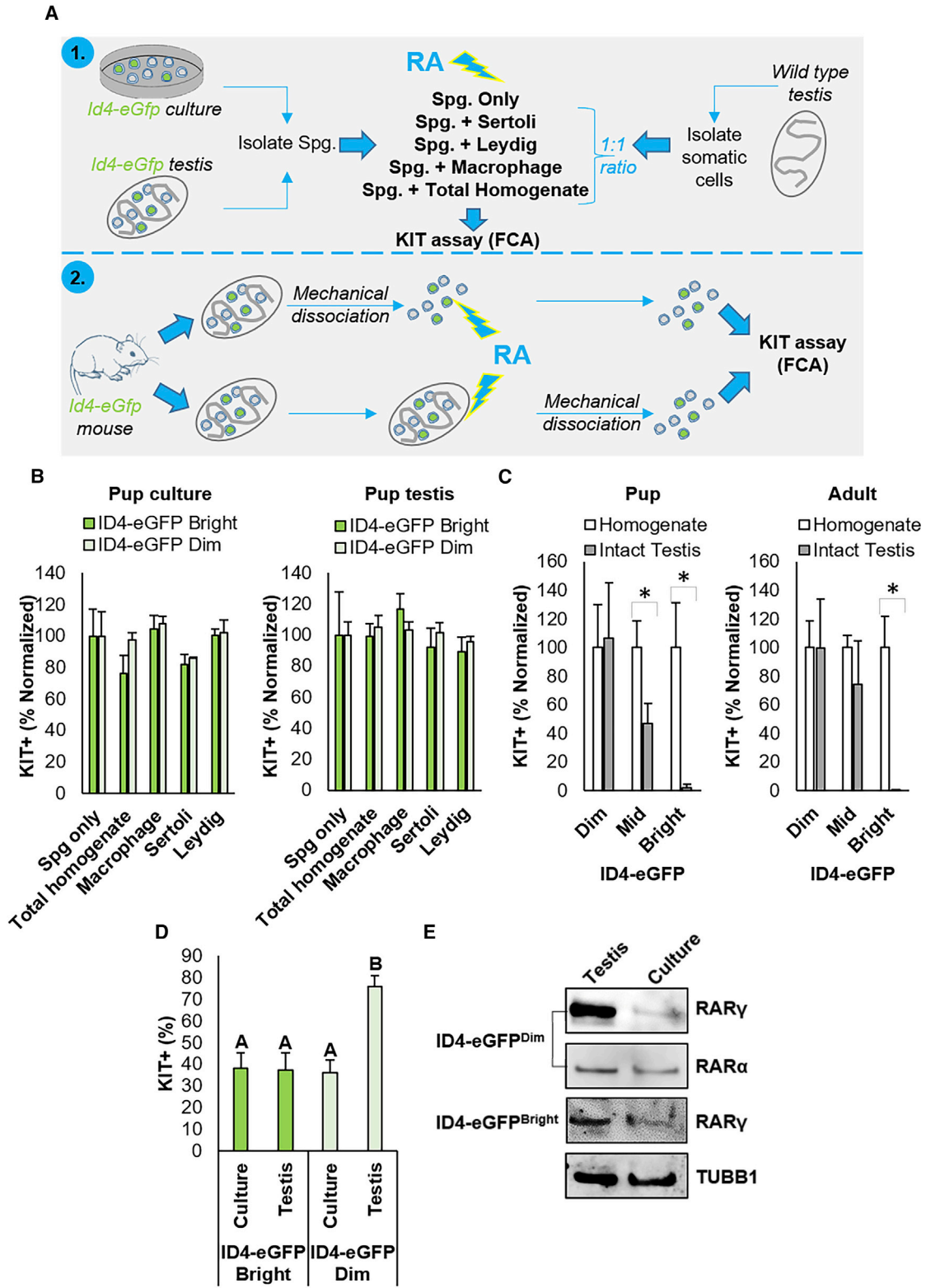


Figure 5. Influence of the Testicular Soma on Modulation of the RA Response in SSC and Progenitor Spermatogonia

(A) Experimental scheme for examining the influence of different testicular somatic cell populations and topographic architecture on RA responsiveness of SSC and progenitor spermatogonia using KIT flow cytometric analysis (FCA).

(legend continued on next page)



cultures and 230 ± 35.5 colonies/ 10^5 cells for adult cultures). Collectively, these data demonstrate that direct exposure to RA outside of the *in vivo* microenvironment elicits a response in SSCs that alters their functional state by pushing them toward differentiation.

The Role of the Soma in Modulating the RA-Induced Differentiating Transition

The findings presented above strongly suggest that influences of an *in vivo* niche protect SSCs from the RA signal by either preventing direct exposure or by providing extrinsic signals that activate an intrinsic suppressive mechanism and that these are lacking in the culture conditions we utilized. Our experimental approach to explore this possibility is depicted in Figure 5A. First, we pre-incubated spermatogonia from culture or ID4-eGFP+ spermatogonia isolated from P6–8 testes with different testis somatic cell populations *in vitro*, including Leydig cells, Sertoli cells, F4/80+ testicular macrophages, or a “total testis homogenate,” in which all these cell populations were present. Combined cell types were then exposed directly to RA and assessed for KIT expression via flow cytometry as a readout for activation of the RA signaling response. Although modest fluctuations in the percentage of KIT+ cells could be identified in ID4-eGFP^{Bright} and ID4-eGFP^{Dim} populations from culture and from the testis in response to the presence of these different somatic cell populations (Figure 5B), no somatic cell population was capable of ablating the RA response in SSCs. Next, we explored whether the different spermatogonial subsets respond to RA exposure when located within a normal testicular architecture by treating testes excised from pup and adult mice *in vitro* (Figure 5C). Note that, in these experiments, ID4-eGFP+ spermatocytes were excluded from analyses on adult testis homogenates by preselecting for undifferentiated spermatogonia using E-cadherin antibody labeling (E-cadherin expression profile is depicted in Figure S1). In contrast to exposure as a single-cell suspension, the RA

signaling response in ID4-eGFP^{Bright} cells was ablated in intact testes (Figures 5C and S4B); with a >46-fold reduction in the number of KIT+ cells compared with the ID4-eGFP^{Bright} population in single-cell suspension from the mechanically dissociated contralateral testis ($p < 0.05$, $n = 4$ for pup, $n = 3$ for adult, values in histogram are normalized to the testis homogenate control). The percentage of KIT+ cells was also halved in the ID4-eGFP^{Mid} population in P6–8 intact testes compared with single-cell suspensions ($p < 0.05$). The absence of KIT+ cells in the ID4-eGFP^{Bright} pool from RA-treated intact testes was not due to a lack of penetration of RA, as equivalent numbers of KIT+ spermatogonia were detected in the ID4-eGFP^{Dim} pool regardless of whether the testis was dissociated or not. These trends can also be appreciated in whole-mount immunofluorescence analyses of RA-treated testes in which ID4-eGFP^{Bright}/SSCs are KIT–, while the KIT+ cells are ID4-eGFP^{Dim} or ID4-eGFP– progenitors (Figure S4B).

Finally, we observed that the *in vivo* environment is also important for priming TA progenitors to respond to the RA signal. When exposed directly to RA, the percentage of ID4-eGFP^{Dim} spermatogonia that became KIT+ was halved (76.1% [$\pm 5.0\%$] versus 36.3% [$\pm 5.7\%$]) if these spermatogonia had been subjected to long term *in vitro* culture, rather than treated immediately following isolation from the testis ($p < 0.01$) (Figure 5D). Contrastingly, when exposed directly to RA in a single-cell suspension the percentage of KIT+ cells in the ID4-eGFP^{Bright} population remained constant. To assess whether extrinsic signals *in vivo* “prime” the ID4-eGFP^{Dim} spermatogonia by stimulating upregulation of *Rarg* expression, Western blot analysis was performed on ID4-eGFP^{Dim} and ID4-eGFP^{Bright} populations isolated directly from testes or primary cultures (Figure 5E). While RAR γ levels were equivalent when comparing the two populations of ID4-eGFP^{Bright} cells, expression was markedly greater in the ID4-eGFP^{Dim} population from the testis directly compared with the ID4-eGFP^{Dim} population from primary cultures. A similar

(B) Quantification of the percentage of KIT+ cells in the ID4-eGFP+ spermatogonial population from primary cultures and from P6–8 pup testis combined at a 1:1 ratio with Sertoli cells, Leydig cells, macrophages, or total testis homogenate (containing all somatic cell populations) and treated with RA. ID4-eGFP+ cells not combined with somatic cells (Spg only) were used as a control. Data are mean \pm SEM for $n = 3$ different cultures or animals (biological replicates). The percentage of both ID4-eGFP^{Bright} and ID4-eGFP^{Dim} subpopulations that were KIT+ are shown normalized to the Spg only control value.

(C) Quantification of the percentage of KIT+ cells in the Bright, Mid, and Dim subsets of the ID4-eGFP+ population in dissociated single testicular cell suspensions or intact testes from pup and adult mice that were treated with RA. Data are presented as mean \pm SEM for $n = 3$ different animals (biological replicates). *Significantly different at $p < 0.05$. Data are normalized to the digested testis control.

(D) Quantification of the percentage of KIT+ cells in ID4-eGFP^{Bright}/SSC and ID4-eGFP^{Dim}/progenitor spermatogonial populations isolated from primary undifferentiated spermatogonial cultures or testes directly and exposed to RA. Data are presented as mean \pm SEM for $n = 3$ different cultures or animals (biological replicates). *Significantly different at $p < 0.05$.

(E) Representative images of western blot analysis for expression of RAR γ and RAR α in ID4-eGFP^{Bright}/SSC and ID4-eGFP^{Dim}/progenitor spermatogonial subsets isolated from primary cultures of undifferentiated spermatogonia or testes directly. Tubulin (TUBB1) was used as a loading control.



trend was not identified in comparing levels of RAR α expression (Figure 5E).

Taken together, these findings demonstrate that the topological arrangement of cell types in the testis and unique architecture influence the responsiveness of SSC and TA progenitor spermatogonial populations to the RA-induced differentiating transition. Moreover, these results indicate that discrete niche microenvironments are established by cell-to-cell communication in mammalian testes to modulate extrinsic cues that influence fate decisions of stem cells and progenitors in the male germline.

DISCUSSION

Maintenance of the SSC population in testes is critical for the preservation of male fertility. Indeed, it is from the SSC reservoir that the entirety of spermatogenesis arises in adult life. As such, it is integral that SSCs are not lost to differentiation in response to the RA signal that is released asynchronously throughout seminiferous tubules to drive the A (undifferentiated) to A1 (differentiating) transition in TA progenitor spermatogonia. At present, the mode by which SSCs and progenitor spermatogonia differentially respond to RA while co-residing in a seemingly facultative environment of the seminiferous epithelium is unresolved. Indeed, conflicting reports exist in the peer-reviewed scientific literature about whether the different subsets of spermatogonia express receptors for RA signaling. In studies of Ikami et al. (2015), this phenomenon was attributed to a lack of RAR γ expression in SSCs that is gained upon the progenitor transition, thereby preventing the self-renewing SSCs from responding to the RA signal. In that study, the GFRA1+ and NEUROG3+ spermatogonia were examined in the context of the entire populations being an SSC or progenitor pool, respectively, and expression of RAR γ was reported to be completely absent in GFRA1+ cells but present in NEUROG3+ cells. Although these findings make for an easy explanation for why progenitors respond to RA but SSCs do not, they are inconsistent with previous studies that have reported expression of RAR γ in some GFRA1+ spermatogonia, and that a majority of these cells do indeed retain the capacity to differentiate even in the absence of spermatogonial *Rar* γ expression (Gely-Pernot et al., 2012).

In the current study, we utilized multiple, complementary approaches to demonstrate expression of RAR γ , as well as other RAR/RXR variants, in a spermatogonial population that is highly enriched for SSCs (i.e., ID4-eGFP+ cells) as well as the GFRA1+ population. Further, we discovered that the receptor complement is functionally intact in both SSC and progenitor subsets to elicit hallmark responses of RA signaling, and induce a loss of regenerative

capacity in SSCs. So, why the discrepancy with the findings of Ikami et al. (2015)? One explanation could be that assessment of RAR γ expression in the Ikami et al. study was made using immunostaining analyses, which may not be sensitive enough for detecting expression by all GFRA1+ spermatogonia. Indeed, our Western blotting results on spermatogonia isolated from the testis directly revealed that RAR γ expression is higher in progenitor spermatogonia than SSCs. Thus, based on the immunostaining technique employed, detection of moderate-to-low RAR γ levels within particular cellular subsets may be challenging, and more sensitive techniques are required to uncover the full spectrum of expression among all spermatogonia. In addition, we were able to detect expression of RARs by GFRA1+ spermatogonia using multiple approaches, all of which revealed expression of RAR γ and RAR α . Moreover, we found that direct exposure to RA elicits a hallmark signaling response in both GFRA1+ and ID4-eGFP+ spermatogonia, demonstrating that the receptor complement is functionally intact. These findings suggest that, rather than being protected from RA-induced differentiation by means of differential RAR γ expression, the SSC population is hidden from the RA pulse *in vivo* by intricate and distinct niche microenvironments established by surrounding somatic cells in the testis.

Stem cells of most, if not all, tissues are thought to reside in a niche microenvironment that is comprised of contributions from support cells. In mammalian testes, the SSC-soma interaction is thought to constitute a niche unit that dictates fate decisions of self-renewal or formation of progenitor spermatogonia that no longer inhabit the niche (de Rooij, 2017; Oatley and Brinster, 2012). However, recent studies have proposed that discrete niche microenvironments for SSCs do not exist, rather all spermatogonia inhabit a facultative or open environment within the seminiferous epithelium (Hara et al., 2014). Findings in the current study suggest that the arrangement of cell types within the testis provides an intricate microenvironment for SSCs to protect them from RA-induced differentiation. Indeed, while exogenous RA exposure does not induce KIT expression in the ID4-eGFP^{Bright} SSC population in the architecturally undisturbed testis, a vast majority of the population becomes KIT+ in the contralateral testis that has been mechanically disassociated into a single-cell suspension before RA exposure. Contrastingly, the ID4-eGFP^{Dim} spermatogonia exhibit a robust KIT response in both experimental situations. Thus, the simple presence of the testicular somatic cells is not sufficient to provide a protective environment in which SSCs are shielded from RA-induced differentiation, but rather it is the interconnected microenvironment that they create which provides this protection. Also, the fact that ID4-eGFP^{Dim} spermatogonia respond to RA exposure both within the intact testis and



as a dispersed single-cell suspension, whereas the ID4-eGFP^{Bright} spermatogonia do not, suggests that the populations exist in different microenvironments that receive disparate extrinsic signals from the surrounding somatic support cells. These findings are supported by those recently published by Agrimson et al. (2017), in which live mice were injected with RA, and the effects on the SSC population in the undisturbed testis was assessed. In that study, SSCs in the undisturbed testes of pre-pubertal mice remained protected from differentiation in the presence of excess RA, as demonstrated by spermatogonial transplantation analyses. While stem cell content was unchanged, the percentage of STRA8+ cells in the ID4-eGFP+ population was significantly elevated. Thus, although Agrimson et al. did not compare STRA8 staining in ID4-eGFP^{Bright} versus ID4-eGFP^{Dim} cells, we can predict that this elevated STRA8+ abundance would be attributed to a response in the ID4-eGFP^{Dim} population, as reflected in the current study.

A prominent unanswered question is what are the external signals within the SSC-niche unit microenvironment *in vivo* that curtail the RA response? The most obvious candidates are the CYP26 enzymes that are potent degraders of RA. Both Sertoli cells and germ cells are known to express the *Cyp26a1* and *Cyp26b1* variants, and simultaneous knock down of *Cyp26b1* in Sertoli and germ cells results in a severe subfertility phenotype (Hogarth et al., 2015). Indeed, 96% of tubules are abnormal in these CYP26B1-deficient mice, and a vast majority of tubules possess obvious vacuolization or a complete loss of germ cells by P15 (Hogarth et al., 2015). In addition, simultaneous knock down of *Cyp26b1* and *Cyp26a1* in Sertoli cells specifically results in overabundant and precocious STRA8 expression in the spermatogonial population (Hogarth et al., 2015). Together, these findings suggest that when the capacity for CYP26B1/A1 production in the testis is impaired, the SSC population may no longer be protected from RA-induced differentiation, and, as a consequence, the capacity for continuation of spermatogenesis is lost. Despite this, how production of these enzymes by Sertoli cells could act to degrade RA selectively within microenvironments surrounding SSC populations remains elusive. Certainly, crosstalk between germ cells and Sertoli cells is known to exist to influence gene expression. For example, spermatogonia have been shown to produce ligands such as JAG1 that activate NOTCH signaling in Sertoli cells (Garcia et al., 2017), modulating Sertoli expression of both *Gdnf* and *Cyp26b1* (Garcia et al., 2013, 2017). However, whether differential spermatogonia-somatic cell interactions exist in SSCs versus progenitors, and whether these interactions relate directly to the RA response *in vivo* will need to be defined by future investigation. Promisingly, however, mining of our previously published RNA-seq database (Helsel

et al., 2017b) revealed that expression of the NOTCH ligands *Dll1* and *Dll3*, as well as *Jag1*, is elevated in ID4-eGFP^{Dim} cells compared with ID4-eGFP^{Bright} cells. It should be noted that although low levels of *Cyp26a1* and *Cyp26b1* expression have been detected in ID4-eGFP^{Bright}/SSC and ID4-eGFP^{Dim}/progenitor populations specifically by our previous RNA-seq analyses (Helsel et al., 2017b), differential expression does not appear to exist between these cell types ($p > 0.1$), supporting findings in the current study that demonstrate a lack of intrinsic protective mechanisms against RA in the SSC population. Also, in line with these findings, knockdown *Cyp26* expression in germ cells alone does not impair fertility (Hogarth et al., 2015).

In addition to the influence of the *in vivo* microenvironment provided by normal testicular architecture on maintenance of the SSC pool, we also discovered an important effect on “priming” progenitor spermatogonia for maximal response to RA. Specifically, we found that ID4-eGFP^{Dim}/progenitor spermatogonia isolated directly from the testis possess markedly higher levels of RAR γ expression compared with the contemporary population isolated from primary culture. This elevated level of RAR γ expression apparently increases the sensitivity of these cells to exogenous RA exposure, as demonstrated by a doubling in the percentage of KIT+ cells. This result marries with previous data from Ikami et al. (2015) that showed induction of ectopic expression of RAR γ in GFRA1+ spermatogonia resulted in increased differentiation rates following physiological pulses of RA in all but a subset of spermatogonia (presumably the true SSCs). In the current study, RAR γ levels were unchanged in SSC populations regardless of origin, isolated from the testis directly or from primary cultures of spermatogonia. These findings suggest that extrinsic signals in the testis act on the progenitor spermatogonia specifically to upregulate expression of RAR γ , again supporting the notion for discrete microenvironments within the seminiferous tubules that dictate differential function of SSCs and progenitors. These experiments also highlight insufficiencies in current *in vitro* culture conditions in terms of maintaining progenitors in their true biological state.

In conclusion, we have provided empirical evidence that the current dogma surrounding the RA response in SSCs versus TA progenitor spermatogonia should be revisited. Specifically, we have demonstrated expression of RAR α , RAR γ , RXR α , and RXR β , as well as their functionality in the SSC pool following direct RA exposure; suggesting that a lack of RAR γ expression is unlikely to account for the resistance to RA-induced differentiation that SSCs exhibit *in vivo*. Instead, we have shown that the SSC population only remains protected from RA when the intricate architecture of the of the SSC niche microenvironment remains undisturbed; a situation that cannot be recapitulated by combining SSCs with different testicular somatic cell



populations as a single-cell suspension *in vitro*, even in the presence of the entire complement that is present in the intact testis. Collectively, our findings depict a previously underappreciated role for testis architecture and microenvironments in modulating RA-induced differentiation in spermatogonial populations and provide compelling evidence for intricate niche microenvironments in the mammalian testis that influence fate decisions of SSC and progenitor spermatogonia. Understanding of these systems not only has the potential to be influential on our perception of stem cell niche environments in other tissue types, but may facilitate advances in our knowledge of underlying causes of male infertility, and potentially the development of novel male contraceptive agents based on RA responsiveness.

EXPERIMENTAL PROCEDURES

Animals

All animal procedures were approved by the Washington State Institutional Animal Care and Use Committee. The *Id4-eGfp* transgenic mouse line was described previously (Chan et al., 2014). *Id4-eGfp* mice were crossed with *Rosa26-LacZ* mice (Jackson Laboratories, stock number 112073) to generate donors for the establishment of spermatogonial culture that are suitable for transplantation analyses. Recipients for spermatogonial transplantation were F1 hybrids of C57BL/6J (Jackson Laboratories, stock number 000664) and 129S1/SvImJ (Jackson Laboratories, stock number 112073). F1 hybrids were treated with busulfan (Sigma-Aldrich, MO, USA, B2635) to eliminate endogenous spermatogenesis prior to transplantation, as described previously (Oatley and Brinster, 2006).

Cell Culture

Primary cultures of undifferentiated spermatogonia were generated from double-transgenic *Id4-eGFP;Rosa26-LacZ* hybrid mice that express the LacZ transgene within all germ cells, but express the EGFP transgene only in ID4+ SSCs (Chan et al., 2014; Helsel et al., 2017b). Primary cultures of spermatogonia were established from the magnetic-activated cell sorting (MACS)-sorted THY1+ fraction of testis homogenates of P6–8 or adult mice (~2–4 months of age) as described previously (Helsel et al., 2017a; Kaucher et al., 2012; Oatley and Brinster, 2006). Where cultures were used for experimental replicates, each culture was derived from a different mouse, and was established independently. In these cultures, >90% of SSCs are captured in the ID4-eGFP+ population, while the ID4-eGFP– cells are progenitor spermatogonia that have lost the capacity for self-renewal, but maintain expression of undifferentiated markers such as *Plzf*, *Utf1*, *Lin28*, and *Pou5f1*, as well as germ cell markers such as *Dazl* and *Ddx4* (Chan et al., 2014). Spermatogonial cultures were maintained on mitotically inactivated SIM mouse embryo-derived thioguanine- and ouabain-resistant feeder monolayers (STOs) in mouse serum-free medium (mSFM) supplemented with the growth factors GDNF (20 ng/mL; Peprotech, NJ, USA) and fibroblast growth factor 2 (1 ng/mL; Peprotech).

While mSFM used for P6–8 cultures was constituted exactly as described previously (Kaucher et al., 2012; Kubota et al., 2004a, 2004b), conditions for adult cultures were slightly modified in that the media was devoid of fatty acids (Helsel et al., 2017a). Also, while P6–8 cultures were kept within humidified incubators at 37°C in 5% CO₂ in air, adult cultures were maintained in glycolysis-optimized conditions (Helsel et al., 2017a). Culture media was replaced every second day, and passaging onto fresh feeders was performed every 6–8 days.

For treatment of cultured spermatogonia with all-*trans* RA (0.5 μM) or DMSO (vehicle), the spermatogonial clumps were separated from feeders by gentle pipetting and single-cell suspension generated by trypsin-EDTA digestion followed by exposure for 16 hr (Yang et al., 2013).

Flow Cytometry

For flow cytometric analysis, single-cell suspensions from the testis or from spermatogonial cultures were generated by trypsin-EDTA digestion as described previously (Chan et al., 2014) and analyzed using an Attune NxT Flow Cytometer (Thermo Scientific, MA, USA). For FACS, single-cell suspensions were fractionated using a Sony SH800 machine. Identification and gating of the ID4-eGFP+ and ID4-eGFP– populations from cultures and pup testes was as described previously (Chan et al., 2014). For assessment of ID4-eGFP+ populations from adult mouse testes, undifferentiated spermatogonia were labeled with a fluorescein-conjugated E-cadherin antibody by incubation at a 1:100 dilution (gated off PE/Cy7 isotype control). For KIT labeling to compare DMSO- and RA-treated spermatogonia, cells were incubated in a fluorescein-conjugated antibody at 1:200 dilution. Gating was selected based on an untreated population of undifferentiated spermatogonia from culture that do not express KIT (Yang et al., 2013). A control population in which primary antibody was omitted was also utilized. For GFRA1 labeling, cells were incubated with an unconjugated primary antibody at 1:100 dilution followed by incubation with a fluorescein-conjugated secondary antibody at 1:500 dilution. Gating was selected based on a control population in which primary antibody was omitted. All antibodies utilized for flow cytometry are listed in Table S1. All incubations on conjugated primary antibodies were conducted in DPBSS (Dulbecco's PBS with 0.1% fetal bovine serum, 10 mM HEPES, 10 mM sodium pyruvate, 1 mg/mL glucose, and 1 mg/mL penicillin/streptomycin) for 20 min on ice. GFRA1 primary antibody incubation was in mSFM overnight at 37°C, and secondary incubation was in mSFM for 2 hr at 37°C.

RT-PCR and qRT-PCR

RNA extraction of isolated spermatogonial cells was conducted using TRIzol reagent (Invitrogen, CA, USA) as per the manufacturer's instructions. Extracted RNA was treated with DNase I, and RNA concentration and purity were determined using a NanoDrop 2000 spectrophotometer (Thermo Scientific) prior to reverse transcription using oligo d(T) priming and Superscript III reverse transcriptase (Invitrogen). Integrity of resulting cDNA was confirmed via PCR using primers specific to the housekeeping gene *Gapdh*. Where stated, qRT-PCR was conducted using validated TaqMan probes and an ABI 7500 fast sequence detection system (Applied Biosystems, NY, USA). Transcript abundance was normalized to



the constitutively expressed ribosomal protein S2 (*Rps2*), and calculated using the $2^{-\Delta\Delta C_t}$ formula, as described previously (Yang et al., 2013). Sequences of all primers are provided in Table S2.

Western Blotting

Protein lysates from spermatogonia were collected using RIPA buffer (Thermo Scientific) supplemented with protease inhibitor (Thermo Scientific) and phosphatase inhibitor (Sigma-Aldrich) cocktails. Samples were resolved in 4%–12% Bis-Tris NuPAGE gels using an XCell SureLock Mini-Cell electrophoresis system (Invitrogen) followed by transfer to nitrocellulose membranes. Prior to addition of primary antibodies, nitrocellulose membranes were blocked in either 5% BSA in Tris-buffered saline (TBS) containing 0.1% Tween (TBST), or 5% skim milk in TBST for 1 hr at room temperature. Primary antibodies are listed in Table S1. All primary antibodies were diluted 1:2,000 in either 5% BSA/TBST (RAR α and RXR β) or 5% skim milk/TBST (RAR γ and RXR α), and blots were incubated overnight at 4°C with gentle rocking. On the next day, blots were washed with TBST prior to a 1 hr incubation in secondary antibody (1:2,000 goat anti-rabbit IgG horseradish peroxidase, Santa Cruz Biotechnology) at room temperature. Blots were again washed, then developed using ECL prime chemiluminescence detection reagent (GE Healthcare, PA, USA) and visualization on a LAS 4000 imager (GE Healthcare).

Immunofluorescence Analyses

For immunofluorescent staining, testes were fixed in Bouin's solution and embedded in paraffin followed by cross-sectioning (5 μ m thickness). After de-paraffinization, antigen retrieval was conducted by boiling slides in citraconic anhydride buffer (pH 7.4, 0.5% citraconic anhydride [Sigma-Aldrich] in ultrapure water) for 20 min. Following this, sections were blocked for non-specific antibody staining using 10% donkey serum in PBS for 1 hr at room temperature. The primary/secondary antibodies and dilutions were as described in Table S1. Sections were incubated in primary antibody or control IgG overnight at 4°C, followed by washing in PBS and incubation with fluorescein-conjugated secondary antibody for 2 hr at room temperature. Cross-sections were again washed in PBS, and mounted in ProLong Gold antifade reagent containing DAPI (Invitrogen).

For immunofluorescence analyses of isolated spermatogonial cell suspensions, cells were adhered to poly-lysine-coated cover slips and fixed in 4% paraformaldehyde for 10 min before permeabilization in ice-cold methanol. Non-specific antibody binding was blocked using 10% serum in 3% BSA/PBS, followed by overnight incubation with primary antibody at 4°C. On the next day, coverslips were washed in PBS, followed by incubation with secondary antibodies for 1 hr at room temperature.

Immunostained cross-sections and single cells were visualized using an IX 51 model inverted microscope (Olympus) and digital images were captured using a DP71 digital microscope camera and CellSense software (Olympus, Tokyo, Japan).

For whole-mount imaging, testes were de-tunicated, and seminiferous tubules gently teased apart on a glass slide. Tubules were placed under a coverslip in mounting media (VectaMount AQ, Vector laboratories, CA, USA) and imaged on a Leica TCS SP5 II confocal microscope.

Spermatogonial Transplantation

The relative SSC content of primary spermatogonial cultures was assayed via germ cell transplantation as described previously (Hessel and Oatley, 2017). In brief, an equal number of cells from primary cultures of undifferentiated spermatogonia established from *Id4-eGfp;Rosa26LacZ* mice were treated with 0.5 μ M RA (Sigma-Aldrich) or DMSO (vehicle control) for 16 hr. Single-cell suspensions of the entire culture well (i.e., containing both ID4-EGFP+ and ID4-EGFP- cells) were then collected, washed by centrifugation and then suspended in mSFM at a concentration of 1×10^6 cells/mL for transplantation. For each recipient mouse testis, 10 μ L of cell suspension (equivalent to 10,000 cells) was microinjected into seminiferous tubules via the efferent duct. Assessment of donor-derived spermatogenesis was conducted 2 months post-transplantation by X-Gal staining for *LacZ*-expressing colonies. Colony numbers were quantified using an SZ51 dissecting microscope used to derive relative SSC contents as described previously (Chan et al., 2014; Oatley and Brinster, 2006).

Isolation of Testis Somatic Cell Populations and Recombination with Spermatogonial Subsets

Enriched populations of Sertoli and Leydig cells were isolated from the one testis of several C57BL/6J adult mice (>6 weeks of age) using methodologies described by Chang et al. (2011). Alongside these cell preparations, the contralateral testes were used to generate a heterogeneous “total testis homogenate,” and also for isolation of testicular macrophage populations. To generate a single-cell suspension from the contralateral testis, the tunica albuginea was removed and automated manual dissociation was conducted using a gentleMACS machine (Miltenyi Biotech, Bergisch Gladbach, Germany). Testicular macrophages were isolated using MACS anti-F4/80 microbeads (Miltenyi Biotech), as per the manufacturer's instructions. For experiments where somatic cell populations were recombined with spermatogonial populations, each population was present at a 1:1 ratio. A 1:1 ratio was selected following preliminary experiments in which additional ratios were examined but produced identical outcomes (data not shown). It should be noted that the “total testis homogenate” provided a control in which normal spermatogonia to somatic cell ratios were maintained, allowing further confirmation that the trends being identified were biologically relevant.

In experiments where RA treatment was conducted using intact testes, the tunica albuginea was removed and the testis placed in 1 mL mSFM with growth factors and 0.5 μ M RA. The contralateral testis was dissociated using gentleMACS and the total homogenate was also re-suspended in 1 mL of the mSFM/RA solution. For these experiments, RA incubation was for 4 hr to limit the impact of degeneration of the testicular tissue that would occur with a longer incubation period.

Statistical Analyses

All experiments were replicated at least three times with different biological samples. Data are presented as the mean \pm SEM for the replicates. Differences between means of treatment groups was determined statistically using the one-way ANOVA or t test function of GraphPad Prism 6 software (La Jolla, CA, USA). Multiple comparison analysis was carried out using the Tukey's *post-hoc*



test function of GraphPad. A value of $p < 0.05$ was considered to be statistically significant.

SUPPLEMENTAL INFORMATION

Supplemental Information includes five figures and two tables and can be found with this article online at <https://doi.org/10.1016/j.stemcr.2018.01.003>.

AUTHOR CONTRIBUTIONS

Conceptualization, T.L. and J.M.O.; Methodology, T.L. and J.M.O.; Investigation, T.L., M.J.O., and J.M.O.; Writing – Original Draft, T.L. and J.M.O.; Writing – Review & Editing, T.L. and J.M.O.; Funding Acquisition, J.M.O.

ACKNOWLEDGMENTS

This research was supported by grant HD061665 awarded to J.M.O. from the NICHD. T.L. is the recipient of the Lalor Foundation Postdoctoral Fellowship. The authors wish to thank Ryan D. Anderson for his assistance in immunofluorescence experiments.

Received: November 21, 2017

Revised: January 4, 2018

Accepted: January 5, 2018

Published: February 1, 2018

REFERENCES

- Agrimson, K.S., Oatley, M.J., Mitchell, D., Oatley, J.M., Griswold, M.D., and Hogarth, C.A. (2017). Retinoic acid deficiency leads to an increase in spermatogonial stem number in the neonatal mouse testis, but excess retinoic acid results in no change. *Dev. Biol.* *432*, 229–236.
- Buageaw, A., Sukhwani, M., Ben-Yehudah, A., Ehmcke, J., Rawe, V.Y., Pholpramool, C., Orwig, K.E., and Schlatt, S. (2005). GDNF family receptor alpha1 phenotype of spermatogonial stem cells in immature mouse testes. *Biol. Reprod.* *73*, 1011–1016.
- Chan, F., Oatley, M.J., Kaucher, A.V., Yang, Q.-E., Bieberich, C.J., Shashikant, C.S., and Oatley, J.M. (2014). Functional and molecular features of the Id4+ germline stem cell population in mouse testes. *Genes Dev.* *28*, 1351–1362.
- Chang, Y.-F., Lee-Chang, J.S., Panneerdoss, S., MacLean, J.A., and Rao, M.K. (2011). Isolation of Sertoli, Leydig, and spermatogenic cells from the mouse testis. *Biotechniques* *51*, 341–344.
- de Rooij, D.G. (2017). The nature and dynamics of spermatogonial stem cells. *Development* *144*, 3022–3030.
- Ebata, K.T., Zhang, X., and Nagano, M.C. (2005). Expression patterns of cell-surface molecules on male germ line stem cells during postnatal mouse development. *Mol. Reprod. Dev.* *72*, 171–181.
- Garcia, T.X., DeFalco, T., Capel, B., and Hofmann, M.-C. (2013). Constitutive activation of NOTCH1 signaling in Sertoli cells causes gonocyte exit from quiescence. *Dev. Biol.* *377*, 188–201.
- Garcia, T.X., Parekh, P., Gandhi, P., Sinha, K., and Hofmann, M. (2017). The NOTCH ligand JAG1 regulates GDNF expression in Sertoli cells. *Stem Cells Dev.* *26*, 585–598.
- Gely-Pernot, A., Raverdeau, M., Célébi, C., Dennefeld, C., Feret, B., Klopfenstein, M., Yoshida, S., Ghyselinck, N.B., and Mark, M. (2012). Spermatogonia differentiation requires retinoic acid receptor γ . *Endocrinology* *153*, 438–449.
- Gely-Pernot, A., Raverdeau, M., Teletin, M., Vernet, N., Féret, B., Klopfenstein, M., Dennefeld, C., Davidson, I., Benoit, G., Mark, M., et al. (2015). Retinoic acid receptors control spermatogonia cell-fate and induce expression of the SALL4A transcription factor. *PLoS Genet.* *11*, e1005501.
- Ghyselinck, N.B., Dupé, V., Dierich, A., Messaddeq, N., Garnier, J.M., Rochette-Egly, C., Chambon, P., and Mark, M. (1997). Role of the retinoic acid receptor beta (RARbeta) during mouse development. *Int. J. Dev. Biol.* *41*, 425–447.
- Grisanti, L., Falciatori, I., Grasso, M., Dovere, L., Fera, S., Muciaccia, B., Fuso, A., Berno, V., Boitani, C., Stefanini, M., et al. (2009). Identification of spermatogonial stem cell subsets by morphological analysis and prospective isolation. *Stem Cells* *27*, 3043–3052.
- Hara, K., Nakagawa, T., Enomoto, H., Suzuki, M., Yamamoto, M., Simons, B.D., and Yoshida, S. (2014). Mouse spermatogenic stem cells continually interconvert between equipotent singly isolated and syncytial states. *Cell Stem Cell* *14*, 658–672.
- Helsel, A.R., and Oatley, J.M. (2017). Transplantation as a quantitative assay to study mammalian male germline stem cells. *Methods Mol. Biol.* *1463*, 155–172.
- Helsel, A.R., Oatley, M.J., and Oatley, J.M. (2017a). Glycolysis-optimized conditions enhance maintenance of regenerative integrity in mouse spermatogonial stem cells during long-term culture. *Stem Cell Rep.* *8*, 1430–1441.
- Helsel, A.R., Yang, Q.-E., Oatley, M.J., Lord, T., Sablitzky, F., and Oatley, J.M. (2017b). ID4 levels dictate the stem cell state in mouse spermatogonia. *Development* *144*, 624–634.
- Hogarth, C.A., Evans, E., Onken, J., Kent, T., Mitchell, D., Petkovich, M., and Griswold, M.D. (2015). CYP26 enzymes are necessary within the postnatal seminiferous epithelium for normal murine spermatogenesis. *Biol. Reprod.* *93*, 19.
- Huckins, C. (1971). The spermatogonial stem cell population in adult rats. 3. Evidence for a long-cycling population. *Cell Tissue Kinet.* *4*, 335–349.
- Ikami, K., Tokue, M., Sugimoto, R., Noda, C., Kobayashi, S., Hara, K., and Yoshida, S. (2015). Hierarchical differentiation competence in response to retinoic acid ensures stem cell maintenance during mouse spermatogenesis. *Development* *142*, 1582–1592.
- Kaucher, A.V., Oatley, M.J., and Oatley, J.M. (2012). NEUROG3 is a critical downstream effector for STAT3-regulated differentiation of mammalian stem and progenitor spermatogonia. *Biol. Reprod.* *86*, 1–11.
- Kent, T., Arnold, S.L., Fasnacht, R., Rowsey, R., Mitchell, D., Hogarth, C.A., Isoherranen, N., and Griswold, M.D. (2015). ALDH enzyme expression is independent of the spermatogenic cycle, and their inhibition causes misregulation of murine spermatogenic processes. *Biol. Reprod.* *94*, 12.
- Kubota, H., Avarbock, M.R., and Brinster, R.L. (2004a). Culture conditions and single growth factors affect fate determination of mouse spermatogonial stem cells. *Biol. Reprod.* *71*, 722–731.



- Kubota, H., Avarbock, M.R., and Brinster, R.L. (2004b). Growth factors essential for self-renewal and expansion of mouse spermatogonial stem cells. *Proc. Natl. Acad. Sci. USA* *101*, 16489–16494.
- Li, H., Palczewski, K., Baehr, W., and Clagett-Dame, M. (2011). Vitamin A deficiency results in meiotic failure and accumulation of undifferentiated spermatogonia in prepubertal mouse testis. *Biol. Reprod.* *84*, 336–341.
- Lord, T., and Oatley, J.M. (2017). A revised A_{single} model to explain stem cell dynamics in the mouse male germline. *Reproduction* *154*, R55–R64.
- Oakberg, E.F. (1971). Spermatogonial stem-cell renewal in the mouse. *Anat. Rec.* *169*, 515–531.
- Oatley, J.M., and Brinster, R.L. (2006). Spermatogonial stem cells. In *Methods in Enzymology*, K. Irina and L. Robert, eds. (Academic Press), pp. 259–282.
- Oatley, J.M., and Brinster, R.L. (2012). The germline stem cell niche unit in mammalian testes. *Physiol. Rev.* *92*, 577–595.
- Tegelenbosch, R.A.J., and de Rooij, D.G. (1993). A quantitative study of spermatogonial multiplication and stem cell renewal in the C3H/101 F1 hybrid mouse. *Mutat. Res.* *290*, 193–200.
- Tong, M., Yang, Q., Davis, J.C., and Griswold, M.D. (2013). Retinol dehydrogenase 10 is indispensable for spermatogenesis in juvenile males. *Proc. Natl. Acad. Sci. USA* *110*, 543–548.
- van Pelt, A.M., and de Rooij, D.G. (1990). Synchronization of the seminiferous epithelium after vitamin A replacement in vitamin A-deficient mice. *Biol. Reprod.* *43*, 363–367.
- Wolbach, S.B., and Howe, P.R. (1925). Tissue changes following deprivation of fat-soluble a vitamin. *J. Exp. Med.* *42*, 753–777.
- Yang, Q., Racicot, K.E., Kaucher, A.V., Oatley, M.J., and Oatley, J.M. (2013). MicroRNAs 221 and 222 regulate the undifferentiated state in mammalian male germ cells. *Development* *140*, 280–290.
- Yoshida, S., Takakura, A., Ohbo, K., Abe, K., Wakabayashi, J., Yamamoto, M., Suda, T., and Nabeshima, Y. (2004). Neurogenin3 delineates the earliest stages of spermatogenesis in the mouse testis. *Dev. Biol.* *269*, 447–458.